Article

Cell Stem Cell

Complete Meiosis from Embryonic Stem Cell-Derived Germ Cells In Vitro

Graphical Abstract

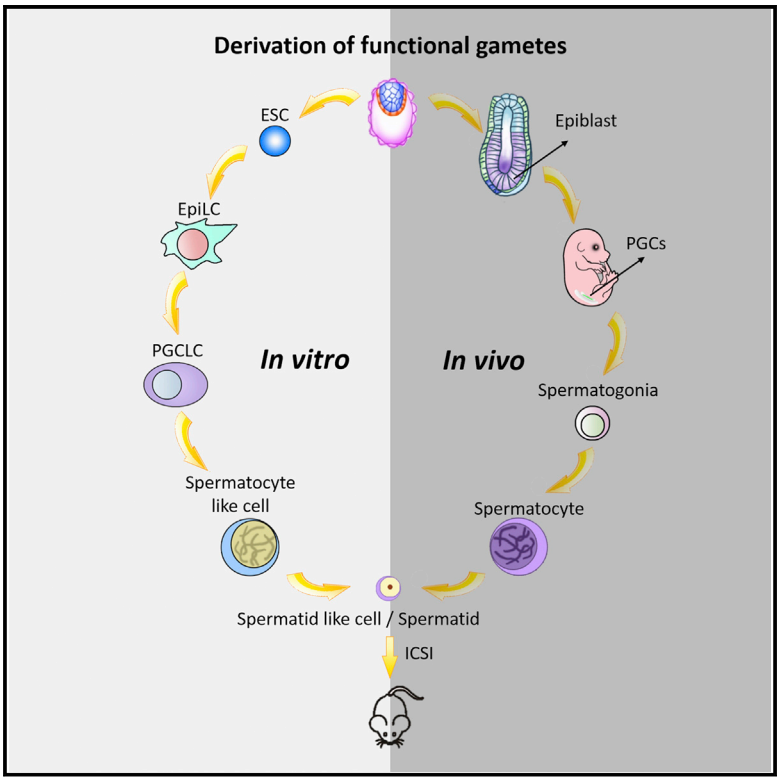

Highlights

- Haploid spermatid-like cells (SLCs) were derived by stepwise differentiation of ESCs
- This process completely recapitulated meiosis in vitro, meeting meiotic hallmarks
- Intracytoplasmic injection of SLCs produced euploid and fertile offspring

Authors

Quan Zhou, Mei Wang, Yan Yuan, ..., Xiao-Yang Zhao, Jiahao Sha, Qi Zhou

Correspondence

qzhou@ioz.ac.cn (Q.Z.),
shajh@njmu.edu.cn (J.S.),
zhaoxiaoyang@smu.edu.cn (X.-Y.Z.)

In Brief

In vitro production of haploid gametes could provide a treatment for infertility, but recapitulating meiosis in culture is a significant roadblock. Zhou et al. report the generation of haploid male gametes from mouse ESCs that can produce viable and fertile offspring, demonstrating functional reproduction of meiosis in vitro.

Accession Numbers

GSE71478
GSE76238

Zhou et al., 2016, Cell Stem Cell *18*, 1–11
March 3, 2016
http://dx.doi.org/10.1016/j.stem.2016.01.017

CellPress

Cell Stem Cell
Article

Complete Meiosis from Embryonic Stem Cell-Derived Germ Cells In Vitro

Quan Zhou,[1,2,8] Mei Wang,[2,3,8] Yan Yuan,[1,2,8] Xuepeng Wang,[2,4] Rui Fu,[2] Haifeng Wan,[2] Mingming Xie,[2,5] Mingxi Liu,[1] Xuejiang Guo,[1] Ying Zheng,[6] Guihai Feng,[2] Qinghua Shi,[7] Xiao-Yang Zhao,[2,9,*] Jiahao Sha,[1,*] and Qi Zhou[2,*]
[1]State Key Laboratory of Reproductive Medicine, Department of Histology and Embryology, Nanjing Medical University, Nanjing 210029, China
[2]State Key Laboratory of Stem Cell and Reproductive Biology, Institute of Zoology, Chinese Academy of Sciences, Beijing 100101, China
[3]College of the Life Sciences, Hunan Normal University, Changsha, Hunan 410081, China
[4]University of the Chinese Academy of Sciences, Beijing 100049, China
[5]College of Life Science, Anhui University of China, Hefei 230601, China
[6]Department of Histology and Embryology, Medical College of Yangzhou University, Yangzhou 225001, Jiangsu, China
[7]Molecular and Cell Genetics Laboratory, Chinese Academy of Sciences Key Laboratory of Innate Immunity and Chronic Disease, Hefei National Laboratory for Physical Sciences at Microscale and School of Life Sciences, University of Science and Technology of China, Hefei 230027, China
[8]Co-first author
[9]Present address: Department of Developmental Biology, School of Basic Medical Sciences, Southern Medical University, Guangzhou 510515, China
*Correspondence: qzhou@ioz.ac.cn (Q.Z.), shajh@njmu.edu.cn (J.S.), zhaoxiaoyang@smu.edu.cn (X.-Y.Z.)
http://dx.doi.org/10.1016/j.stem.2016.01.017

SUMMARY

In vitro generation of functional gametes is a promising approach for treating infertility, although faithful replication of meiosis has proven to be a substantial obstacle to deriving haploid gamete cells in culture. Here we report complete in vitro meiosis from embryonic stem cell (ESC)-derived primordial germ cells (PGCLCs). Co-culture of PGCLCs with neonatal testicular somatic cells and sequential exposure to morphogens and sex hormones reproduced key hallmarks of meiosis, including erasure of genetic imprinting, chromosomal synapsis and recombination, and correct nuclear DNA and chromosomal content in the resulting haploid cells. Intracytoplasmic injection of the resulting spermatid-like cells into oocytes produced viable and fertile offspring, showing that this robust stepwise approach can functionally recapitulate male gametogenesis in vitro. These findings provide a platform for investigating meiotic mechanisms and the potential generation of human haploid spermatids in vitro.

INTRODUCTION

In sexually reproducing organisms, transmission of genetic and epigenetic information between generations relies on gametes, reproductive cells of the germline that unite at fertilization to form a new organism. In mammals, germline specification occurs early during embryogenesis, when primordial germ cells (PGCs) first appear in the extra-embryonic compartment. These germ cell progenitors undergo a complex developmental program involving migration into the developing embryo, colonization of the gonadal ridges, proliferation, and eventual progression through meiosis to form haploid sex-specific germ cells. Up to 15% of couples are infertile, and many of them have gametogenesis failure. Therefore, reproducing germ cell development in vitro has remained a central goal in reproductive biology and medicine (Sun et al., 2014). The effective production of functional gametes in culture would not only provide a system to investigate the genetic, epigenetic, and environmental factors that shape germ cell development but may also lead to clinical approaches addressing infertility resulting from defects in gametogenesis.

The recapitulation of meiosis, a process unique to germ cells, has remained a major obstacle toward the production of functional gametes in vitro. To avoid misconceptions, a consensus panel of reproductive biologists has therefore formulated a panel of "gold standard" criteria for in-vitro-derived gametes that are based on features that reflect key events of meiosis (Handel et al., 2014). To prove that meiosis occurred in vitro, all of the following must be shown: correct nuclear DNA content at specific meiotic stages (for male cells, pre-meiotic, meiotic S phase, first reductional, and second meiotic division stages), normal chromosome number and organization, appropriate nuclear and chromosomal localization of proteins involved in homologous synapsis and recombination, and capacity of the in vitro-produced germ cells to produce viable euploid offspring.

The production of mature male germ cells is the result of a complex developmental program that begins with the specification of PGCs during prenatal stages and relies on spermatogenesis, a complex multi-step expansion and maturation process that is initiated in the postnatal testis during puberty and encompasses mitotic proliferation of spermatogonia, meiotic division into haploid germ cells, and spermiogenic differentiation. In response to cytokines resembling those released by early extraembryonic tissues, mouse and human embryonic stem cells (ESCs) or induced pluripotent stem cells

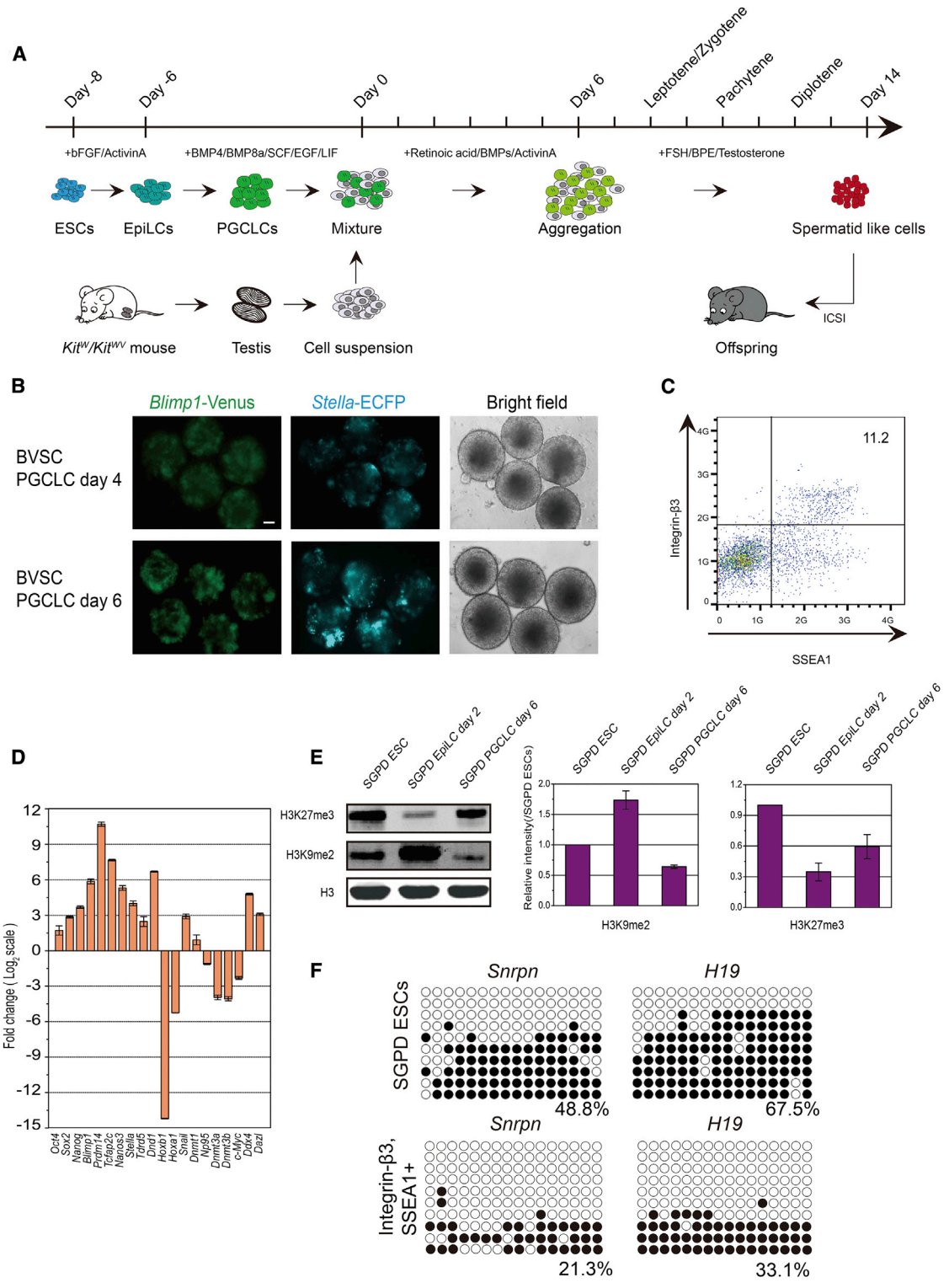

Figure 1. SGPD and BVSC ESCs Differentiated into PGCLCs

(A) Time line and culture conditions of in vitro spermatogenesis.

(B) Expression of *Blimp1*-mVenus and *Stella*-ECFP identifies BVSC ESC-derived PGCLCs on days 4 and 6 of PGCLC culture (days −2 and 0 of overall culture). Scale bar, 50 μm.

(C) FACS of SSEA1 and integrin β3 double-positive cells in day 6 aggregates (day −2).

(legend continued on next page)

(iPSCs) can adopt an epiblast-like developmental program in vitro and transiently form epiblast-like cells (EpiLCs) that are competent to undergo specification into PGC-like cells (PGCLCs) (Hayashi et al., 2011; Irie et al., 2015). Upon transplantation of murine PGCLCs into the testis environment, these further developed into haploid spermatozoa (Hayashi et al., 2011). In humans, the risk for tumorigenesis prohibits in vivo transplantation approaches so that the capacity of human PGCLCs to form spermatozoa remains unexplored. Several studies have reported the generation of haploid germ cells in vitro from pluripotent stem cells (Eguizabal et al., 2011; Geijsen et al., 2004), but none of these studies provided proof for all key hallmarks of meiosis, and the functionality of the haploid germ cells were not fully evaluated. A 3D culture system aimed at reconstructing mouse seminiferous tubules in vitro supported sperm formation from neonatal testicular cells. However, the function of the spermatids obtained with this system has not been evaluated (Yokonishi et al., 2013). Therefore, the full recapitulation of spermatogenesis in vitro to produce functional haploid male gametes has not yet been achieved but is highly anticipated.

Here we report complete in vitro meiosis from murine ESC-derived PGCLCs, resulting in the formation of male spermatid-like cells (SLCs) capable of producing viable fertile offspring via intracytoplasmic sperm injection (ICSI). We demonstrate that, upon co-culture with neonatal testicular somatic cells and sequential exposure to morphogens and sex hormones, ESC-derived PGCLCs recapitulate male gametogenesis in vitro, reproducing hallmarks of erasure of imprints, synapsis, and recombination.

RESULTS

Specification of PGCLCs from ESCs In Vitro

To visualize key stages during germ cell development from ESCs in vitro, we derived and used mouse ESC lines transgenic for fluorescent reporter proteins under the control of regulatory elements of germ cell markers. For identification of cells resembling PGCs, we used an ESC line expressing membrane-targeted Venus (mVenus) under the control of *Prdm1* (*Blimp1*) regulatory elements and enhanced CFP (ECFP) under the control of *Dppa3* (*Stella*/*Pgc7*), marking lineage-restricted PGC precursors of the proximal epiblast and Prdm1- and Dppa3-positive migrating PGCs, respectively (*Blimp1*-mVenus and *Stella*-ECFP [BVSC] double-transgenic ESC line). We also used an ESC line expressing EGFP controlled by the cell-specific stimulated by retinoic acid gene 8 (*Stra8*) promoter, reflecting early-stage spermatogonia through preleptotene-stage spermatocytes (Li et al., 2007). This line also expressed DsRed under the control of the protamine 1 (*Prm1*) promoter, identifying post-meiotic spermatids (*Stra8*-EGFP and *Prm1*-DsRed [SGPD] double-transgenic ESC line; Figure S1A). Both ESC lines had a normal karyotype and produced completely ESC-derived live offspring by tetraploid complementation (Figures S1B and S1C), confirming pluripotency.

From ground-state SGPD and BVSC ESCs that were maintained under serum- and feeder free conditions in the presence of GSK3 inhibitor and MEK inhibitor (2i) and leukemia inhibitory factor (LIF), we first induced differentiation into EpiLCs using culture conditions adapted from a protocol published previously (Hayashi et al., 2011). In adherent culture, SGPD and BVSC ESCs underwent EpiLC differentiation when exposed to activin A and basic fibroblast growth factor (bFGF) (Figure 1A). This fate change was associated with a decrease in the expression of the pluripotency markers NANOG and SOX2, whereas levels of the pluripotency and germ cell marker OCT4 remained high (Figure S2A). Expression analysis by real-time RT-PCR confirmed downregulation of transcripts of multiple pluripotency and inner cell mass (ICM) marker genes, including *Prdm14*, *Zfp42*, *Tbx3*, *Tcl1*, *Esrrb*, *Klf2*, *Klf4*, and *Klf5*, whereas transcripts of the epiblast marker genes *Fgf5* and *Wnt3* and of *Dnmt3b* became upregulated (Figure S2B). Transcripts of endoderm marker genes (*Gata4*, *Gata6*, *Sox17*, and *Blimp1*) were expressed at low levels during differentiation.

Subsequent floating culture of EpiLC in an N2B27-based differentiation medium containing a cytokine mix of BMP-4, BMP-8a, epidermal growth factor (EGF), SCF, and LIF (Hayashi et al., 2011) resulted in robust activation of *Blimp1*-mVenus and *Stella*-ECFP after 4–6 days, suggesting induction of PGCLCs (Figure 1B). Fluorescence-activated cell sorting (FACS) for the PGC markers integrin β3 and SSEA1 yielded 11.2% double-positive cells (Figure 1C). We next evaluated whether changes in gene expression, histone modification, and allele-specific methylation patterns associated with PGC commitment were recapitulated in our culture system. Comparison of expression profiles of SGPD ESC-derived EpiLCs and day 6 PGCLC aggregates revealed upregulation of transcripts of pluripotency genes, including *Oct4*, *Sox2*, and *Nanog*, in PGCLCs (Figure 1D). Similarly, transcript levels of PGC-related genes, including *Blimp1*, *Prdm14*, *Tcfap2c, Nanos3*, *Stella*, *Tdrd5*, *Dnd1*, *Dnmt1*, *Ddx4*, and *Dazl*, increased, whereas those of somatic cell-related genes such *hoxa1* and *hoxb1* and other genes, including *Dnmt3a*/*3b*, *Np95*, and *c-Myc*, became downregulated. This gene expression profile resembles that of in vivo PGCs (Kurimoto et al., 2008; Saitou et al., 2002), confirming in vitro PGCLC specification (Hayashi et al., 2011). Analysis of epigenetic profiles by western blot demonstrated similar dynamics of histone modification as observed during PGC formation in vivo (Seki et al., 2005) and PGCLC induction in vitro, with a transient increase and reduction of histone H3 lysine 9 dimethylation (H3K9me2) and histone H3 lysine 27 trimethylation (H3K27me3), respectively, during formation of EpiLCs, followed

(D) Gene expression changes in SGPD PGCLCs between day 0 (day −2 of overall culture) and day 6 of PGCLC culture (day 0). Average values ± SD were plotted on the $\log_2$ scale.

(E) Western blot analysis (left) of H3K9me2 and H3K27me3 in SGPD ESCs, SGPD day 2 EpiLCs (day −6 overall), and SGPD day 6 (day 0 overall) PGCLCs (SSEA1 and integrin β3 double-positive cells). Quantification of H3K9me2 (center) andH3K27me3 normalized to H3 levels (right); mean ± SD.

(F) Bisulfite sequencing of DMRs that regulate mono-allelic expression of the imprinted genes *Snrpn* and *H19* from the paternal and maternal allele, respectively. White and black circles indicate unmethylated and methylated CpGs, respectively.

See also Figures S1 and S2.

by the inverse pattern in PGCLCs (Figure 1E; Hayashi et al., 2011; Seki et al., 2005). Bisulfite sequencing of differentially methylated regions (DMRs) that regulate mono-allelic expression of the imprinted genes *Snrpn* and *H19* from the paternal and maternal allele, respectively, revealed a reduction of methylation that may indicate that erasure of imprinting was initiated in SGPD PGCLCs (Figure 1F). Collectively, both SGPD and BVSC ESCs were induced effectively to form PGCLCs.

Initiation of Meiosis in PGCLCs In Vitro in Co-culture

Completion of spermatogenesis from in vitro-produced PGCLCs has only been achieved after transplantation into mouse testes using the germ cell-deficient KIT^{W}/KIT^{W-V} mouse model to ensure the donor origin of haploid cells (Hayashi et al., 2011). To reconstitute an in vitro environment compatible with meiotic progression, we pursued co-culture of PGCLCs with early postnatal testicular cells from KIT^{W}/KIT^{W-V} mice. In male mice, fetal-stage gonadal somatic cells express high levels of CYP26B1, which metabolizes endogenous retinoic acid (RA), thereby prohibiting entry of male germ cells into meiosis (Bowles et al., 2006; MacLean et al., 2007). Initiation of meiosis remains suppressed in the male gonad until after birth (Zhou et al., 2008). Consistent with this, we found that early postnatal somatic testicular cells express low levels of CYP26B1, comparable with those of the female fetal gonad at the stage of meiotic induction of PGCs at embryonic day (E) 13.5 (Anderson et al., 2008; McLaren, 2003; Figure S3A). Therefore, early postnatal testicular cells of KIT^{W}/KIT^{W-V} mice may represent a permissive environment for the initiation of meiosis (Zhou et al., 2008) despite developmental asynchrony. We used a mixed cell culture system of SGPD PGCLCs and KIT^{W}/KIT^{W-V} testicular cells at a ratio of 1:1.

An RA signal is required during meiotic induction (Bowles et al., 2006; Menke et al., 2003; Zhou et al., 2008), and pathways responsive to activin A and BMP-2/4/7 (BMPs) regulate postnatal germ cell development, including self-renewal (Hu et al., 2004; Puglisi et al., 2004). To assess the effect of these morphogens on the initiation of meiosis in vitro, we exposed co-cultures of SSEA1 and integrin β3 double-positive PGCLCs and KIT^{W}/KIT^{W-V} testicular cells to different combinations of activin A, BMPs, and RA (Figure 1A). Only in cultures supplemented with all three morphogens (activin A, BMPs, and RA) did *Stra8*-EGFP-expressing cells become apparent within 3 days of exposure, suggesting the initiation of meiosis in SGPD PGCLCs in vitro (Figure 2A). Gene expression analysis revealed that increased transcript levels of the germ cell markers *Nanos3* and *Ddx4* were detectable in all cultures exposed to activin A and BMPs. However, only co-cultures additionally supplemented with RA exhibited a marked upregulation of the meiosis markers *Stra8* and *Dmc1* after day 6 (Figure 2B). The expression level of *Rec8*, another target of RA but independent of *Stra8* (Koubova et al., 2014), was higher when treated with RA than that without RA treatment after day 6 (Figure 2B). Cells not exposed to activin A or BMPs exhibited poor proliferation capacity (Figure 2C). In co-cultures exposed to all three morphogens, we observed that testis somatic cells migrated actively toward PGCLCs, forming aggregation colonies with *Stra8*-EGFP-expressing cells within 6 days (Movie S1). *Prm1*-DsRed expression was not detected at this time. 336 of the 400 (84%) colonies showed *Stra8*-EGFP-positive signals. The *Stra8*-EGFP-positive colonies were positive for markers of germ cells (DDX4), testis somatic cells (GATA4), and Sertoli cells (SOX9), whereas the PGC markers SSEA1 and OCT4 were undetectable (Figure 2D). SGPD PGCLCs had therefore differentiated from a PGC/spermatogonial stem cell (SSC) state and integrated into colonies comprised of multiple testicular cell types, including KIT^{W}/KIT^{W-V} testicular somatic cells. In BVSC double-positive PGCLCs, downregulation of the *Blimp1*-mVenus and *Stella*-ECFP signal occurred within 3 days of co-culture in the presence of all three morphogens, supporting this hypothesis (Figure S3B). This synchronous process resembles the behavior of PGCs in the E13.5 female genital ridge, which simultaneously enter meiosis in the following few days. Our co-culture conditions therefore reconstitute a microenvironment that triggers the initiation of meiosis in germ cells.

Hormonal Stimulation Induces the Formation of Haploid SLCs In Vitro

Sex hormones, including follicle-stimulating hormone (FSH) and testosterone (T) regulate the progression of meiosis in mice (O'Shaughnessy, 2014). Starting on day 7 of co-culture, we therefore withdrew morphogens (Activin A, BMRs, and RA [ABR]) and exposed SGPD-derived cultures to combinations of FSH, bovine pituitary extract (BPE), and T. In the presence of FSH/BPE/T, postmeiotic *Prm1*-DsRed-expressing cells became first detectable on day 10 (Figure 3A), and strong reporter expression on day 14 correlated with upregulation of haploid spermatid markers such as *Tp1*, *Prm1*, *acrosin*, and *haprin*. In contrast, cultures supplemented with fewer hormone factors did not contain *Prm1*-DsRed-expressing cells. A slight upregulation of *Sycp3* was detectable in cultures exposed to BPE and T (Figure 3B). In the presence of FSH/BPE/T, 14% of cells were identified to have 1C DNA content on day 14 of culture, indicating the formation of haploid male SLCs. Less than 3% of SLCs were detectable in cultures not exposed to FSH, and SLCs were absent from cultures without BPE or T (Figure 3C), indicating that all three hormones were required for progression of meiosis. No 1C cells could be induced from the somatic cells on day 14, even in the presence of FSH/BPE/T (Figure 3C). In addition to FSH, BPE contains a variety of growth factors and hormones. Therefore, it is possible that factors other than FSH contribute to the observed completion of meiosis in vitro with FSH, T, and BPE stimulation.

In FSH/BPE/T-supplemented cultures, haploid cells were first detectable around day 10 and increased over the next 4 days to 14%–20%. Approximately half of the haploid cells expressed *Prm1*-DsRed on day 14 (Figure 4A). Cells had a normal karyotype during metaphase of meiosis I (Figure 4B).

Chromosome Synapsis and Recombination in Meiosis In Vitro

To observe the progression of meiosis during culture, we assessed chromosomal synapsis and recombination/crossover. These processes require the initiation and resolution of DNA double-strand breaks (DSBs). Nuclear spreads of differentiating cells on day 8 contained multiple SPO11 and RAD51

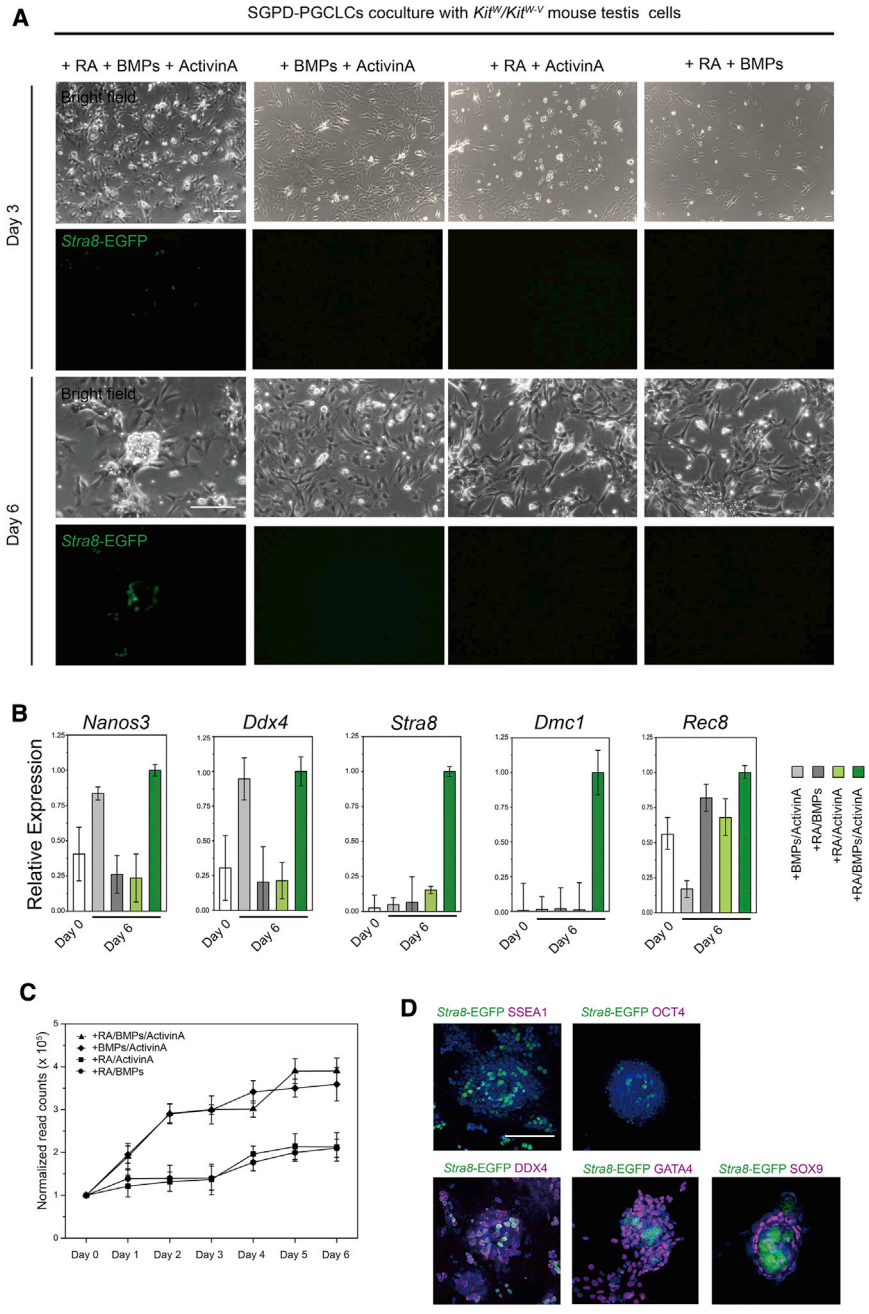

Figure 2. Induction of Meiosis in PGCLCs In Vitro

(A) SGPD-derived PGCLCs initiate meiosis in co-culture with $KIT^{W}/KIT^{W\text{-}V}$ testicular cells when exposed to activin A, BMPs, and RA. *Stra8*-EGFP-positive cells and colonies were detected after 3 and 6 days, respectively. Scale bar, 100 μm.

(B) qRT-PCR of co-cultures exposed to different morphogen combinations. Relative gene expression levels were normalized to Rps2 and reflect mean ± SD from three independent biological replicates.

(C) Mean (± SD) cell counts of cultures. 10^5 cells/well were plated on day 0.

(D) Immunostaining of day 6 colonies with antibodies directed against germ cell and somatic cell markers combined with Hoechst staining (blue) and *Stra8* promoter-driven EGFP expression. Scale bar, 50 μm.

See also Figure S3 and Movie S1.

foci, reflecting the generation of DSBs (Aravind et al., 1998; Keeney et al., 1997) and their resolution by homologous recombination repair (Neale and Keeney, 2006), respectively (Figure 4C; Figures S3C–S3F). Furthermore, we found that the distribution of phosphorylated H2A histone family member X (γH2AX) recapitulated that of meiotic progression in vivo. Broad distribution throughout the nucleus in day 8 cells (Figure 4C; Figure S3C) reflected an association with DSBs, and disappearance from the autosome region on day 10 and accumulation on the unsynapsed sex chromosomes (Mahadevaiah et al., 2001) suggested completion of synapsis similar to pachytene stage spermatocytes in vivo (Figure 4C). The nuclei of in vitro spermatocytes were positive for SYCP1, a component of transverse elements of the synaptonemal complex (Lammers et al., 1994; Meuwissen et al., 1992), and also contained lateral (SYCP3) elements (Eijpe et al., 2000), suggesting progression of synapsis. Quantitative analysis revealed that, after 8 days of differentiation in vitro, more than 90% of the primary spermatocytes were at the leptotene or zygotene stage of meiosis. On day 10, 64% were in the pachytene stage, indicating the successful repair of DNA DSBs and completion of synapsis, and more than 50% of the spermatocytes had entered the diplotene stage by day 12 (Figure 4D). These results demonstrated that meiosis in vitro encompassed synapsis and recombination and was synchronized in the majority of germ cells. Consistent with this, we found that upregulation of transcripts of meiotic factors occurred in a programmed manner, similar to one cycle of meiotic division in vivo (Figure 4E). Transcripts of the meiotic markers *Dmc1* and *Stra8* were first detectable on day 4, increased to the highest levels between days 7 and 10, and decreased by day 14. *Sycp3* transcript levels increased gradually from day 0 to day 10 and then dropped sharply on day 14, consistent with progression to the diplotene stage, and upregulation of haploid spermatid marker transcripts such as *Prm1*, *haprin*, and *acrosin* was most prominent on day 14. FACS of *Prm1*-DsRed-expressing SLCs on day 14 yielded approximately 2×10^4 SLCs/culture well. Because meiotic progression of a single PGCLC would result in four SLCs, the estimated conversion rate from PGCLCs (5×10^4 PGCLCs plated per well) to SLCs was about 10%. Dividing *Prm1*-DsRed-positive cells were present in co-cultures on day 12, indicating the formation of haploid cells (Movie S2).

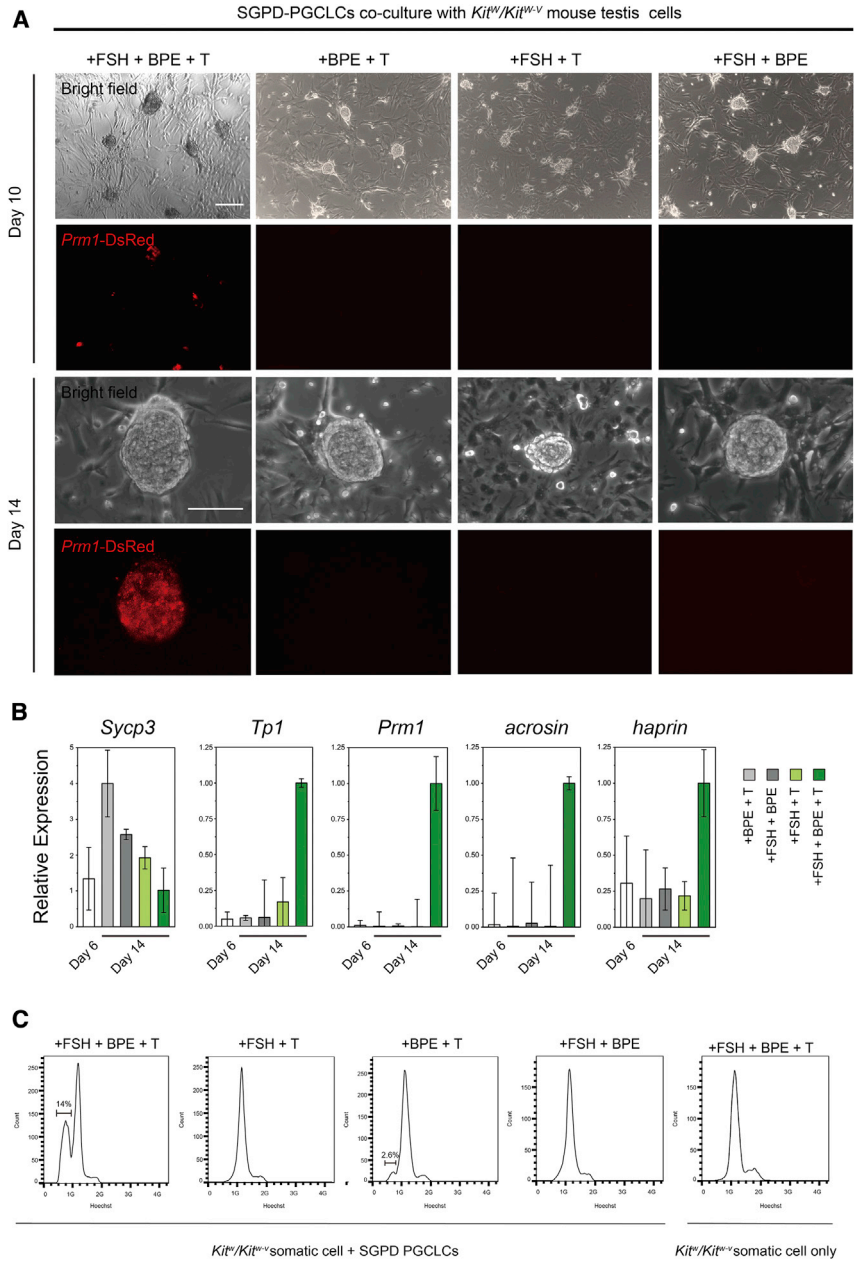

Figure 3. Hormonal Stimulation Induces the Formation of Haploid SLCs in Culture

(A) SGPD-derived co-cultures were supplemented with hormones from days 7–14. *Prm1*-DsRed-expressing cells were detected on day 10 in the presence of FSH/BPE/T. Scale bars, 100 μm.

(B) qRT-PCR analysis of cultures supplemented with hormones as indicated. Relative gene expression levels were normalized to Rps2 and reflect mean ± SD from three independent biological replicates.

(C) FACS analysis of DNA content revealing the presence of 14% and 2.6% haploid SLCs only in cultures exposed to FSH/BPE/T and BPE/T (days 7–14), respectively.

See also Movie S2.

Global transcription profile clustering analyses revealed the similarity of in vitro SLCs to in vivo spermatids (Figure 5D). These analyses also confirmed that global transcription profiles of SSEA1/integrin β3 double-positive PGCLCs on day 6 clustered closely with those of SSEA1/integrin β3 double-positive PGCs from E12.5 male fetuses but differed from ESCs and differentiated germ cells.

We next performed ICSI with sorted in vitro-derived SLCs. Of 63 and 125 oocytes injected with SGPD-derived SLCs in two replicates, 51 and 107 developed to the two-cell stage after activation, respectively. Of 191 oocytes injected with BVSC-derived SLCs, 159 developed to the two-cell stage after activation (Table 1). From embryo transfers of SGPD-derived two-cell stage embryos, we obtained six full-term pups that were transgenic for *Prm1*-DsRed (Figures 5E and 5F). Analysis of one pup revealed a normal karyotype (Figure 5G). Bisulfite sequencing indicated a pattern associated with maternal and paternal genetic contributions (Figure 5H). The mouse developed normally to adulthood. Embryos resulting from ICSI with BVSC-derived SLCs (Figure S5A) expressed *Stella*-ECFP at the four-cell stage (Figure S5B). Embryo transfer resulted in three live pups that were positive for the *Blimp1*-mVenus and *Stella*-ECFP transgenes, had a normal karyotype, and exhibited normal weight gain after birth (Figures S5C–S5F). The birth rate following ICSI with round spermatids isolated from normal testis was 9.5% (Table 1). Genome-wide reduced representation bisulfite sequencing (RRBS) of tail tip fibroblast of a male and a female offspring derived from BVSC ESCs was performed to analyze the whole-genome methylation status of the offspring with normal male and female mice as controls. The genome-wide methylation data of sperm and oocyte by Shen et al. (2014) were included in the analysis. The proportions of high methylation sites (>80%)

Healthy Fertile Offspring Produced by ICSI with In Vitro-Derived SLCs

Sorted SLCs contained a cap-shaped acrosome (Figure 5A). To validate genome integrity, we performed 0.1× whole genome sequencing of single sorted SLCs. Of eight small and round cells selected for sequencing (Figure 5B), six were haploid cells with normal genome structure, one cell was haploid with chromosomal deletions, and one was diploid (Figure S4). The presence of diploid cells was not unexpected because the *Prm1*-DsRed-positive population contained diploid cells (Figure 4A), and we chose not to select cells for DNA content to avoid interference with sequencing. Bisulfite sequencing revealed male germ cell-specific differential methylation at the imprinted *H19* and *Snrpn* loci comparable with that of in vivo round spermatids (Figure 5C).

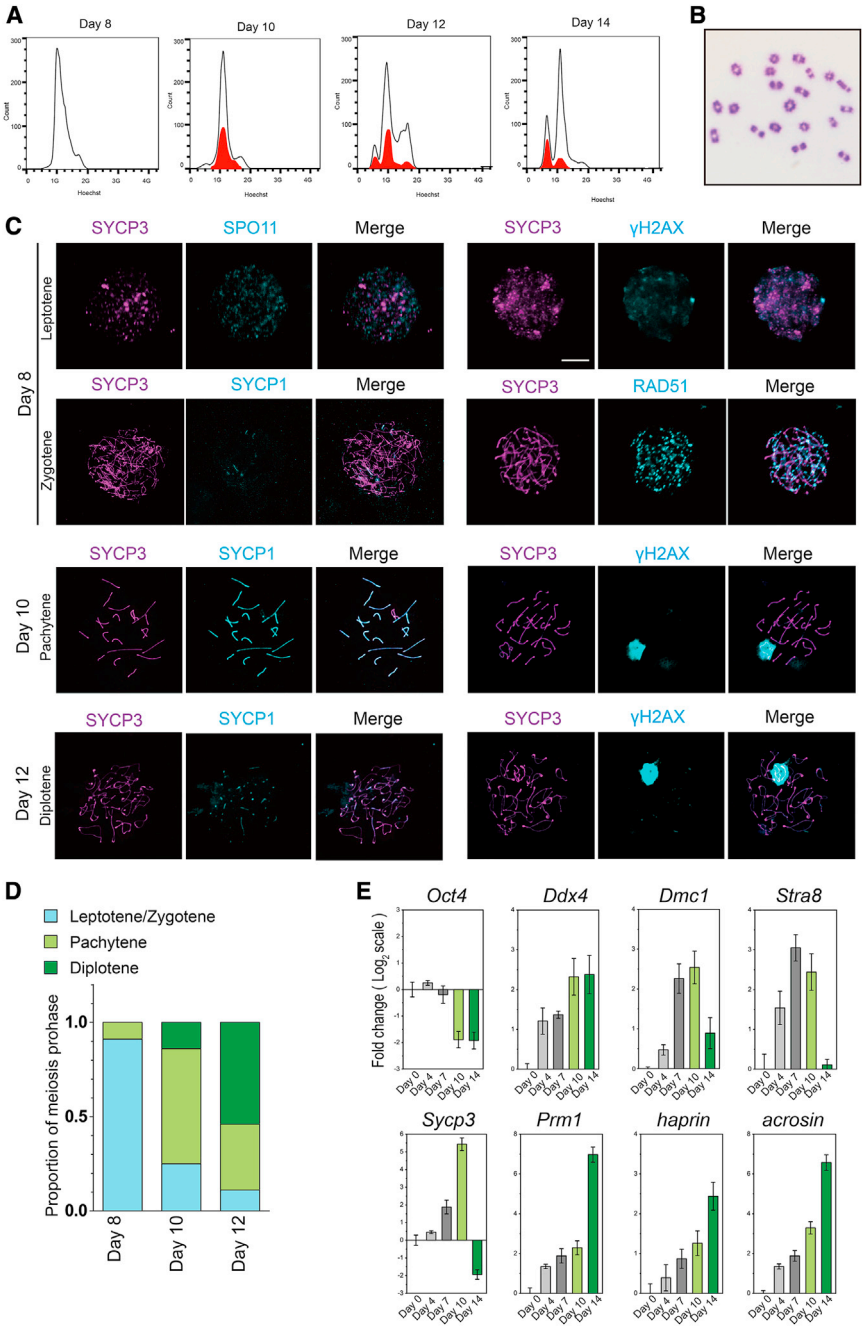

Figure 4. Chromosomal Synapsis and Recombination during In Vitro Meiosis

(A) FACS analysis of DNA contents in spermatogenic cultures from days 8–14. Red histograms reflect *Prm1*-DsRed-positive cells.

(B) Metaphase spread of a day 12 spermatocyte.

(C) Localization of SYCP3, SYCP1, γH2AX, SPO11, and RAD51 in nuclear spreads of germ cells on days 8–12 of co-culture. Scale bar, 100 μm.

(D) Proportion of leptotene/zygotene-, pachytene-, and diplotene-stage spermatocytes in day 8–12 SLCs. The stages were identified according to SYCP3 distribution.

(E) qRT-PCR analysis of cultures from days 0–14. Relative gene expression levels were normalized to Rps2 and reflect mean ± SD from three independent biological replicates.

See also Figure S3.

summary, we describe the successful generation of ESC-derived spermatids in vitro that fully conform to the gold standards proposed for in vitro-derived germ cells (Handel et al., 2014).

DISCUSSION

Here we report the first successful generation of functional spermatids, conforming to the gold standards of in-vitro-derived germ cells, from pluripotent stem cells by stepwise differentiation in vitro. Specifically, we demonstrate that mouse ESC-derived PGCLCs entered meiosis in vitro, undergoing key processes of in vivo meiosis, including chromosomal synapsis and recombination, and finally differentiated into haploid SLCs. These SLCs successfully fertilized oocytes by ICSI, and the resulting embryos underwent embryonic development, resulting in fertile offspring that gave birth to the next generation. This unequivocally demonstrates the recapitulation of meiosis in a culture environment and proves the functionality of spermatids generated from pluripotent stem cells in vitro.

of the BVSC-derived offspring and control mice were all lower than that of sperm but higher than that of the oocyte (Figure S5G), which is consistent with the lower methylation levels of somatic cells. The clustering analysis showed that the BVSC-derived male offspring was clustered together with the male control (Figure S5H). Additionally, imprinting regions from BVSC-derived offspring and control mice were analyzed, and all showed a 50% methylation level (Figure S5I). Therefore, BVSC ESC-derived offspring had a normal methylation level. All of these mice developed to adulthood and had offspring (Figure S5J). These data demonstrate the generation of functional spermatids in vitro from both SGPD and BVSC ESC lines. In

To establish an efficient approach for in vitro meiosis and gametogenesis, we adapted a method used to differentiate EpiLCs into PGCLCs from a protocol published previously (Hayashi et al., 2011) using N2B27 as basal medium for PGCLC induction. N2B27 is a chemically defined medium that contains the RA precursor vitamin A and insulin. This medium supports the ground-state pluripotency of ESCs when supplemented with 2i and is used frequently as a basal medium to promote neural differentiation from pluripotent cells. We presume that continued exposure to N2B27, which constituted the basal

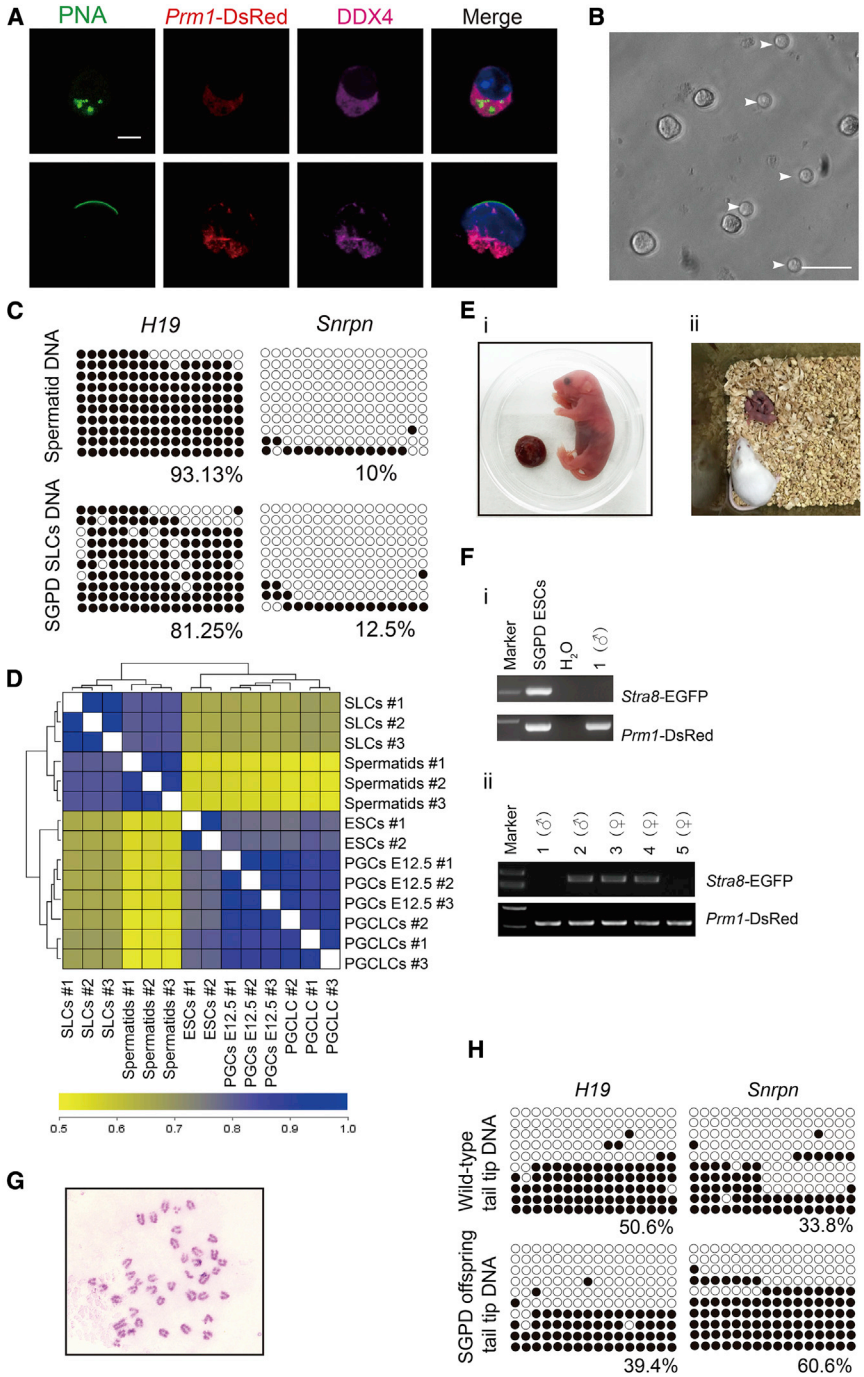

Figure 5. Healthy Offspring Produced from In Vitro-Derived SLCs

(A) Acrosin and PNA staining of SLCs. Scale bar, 5 μm.

(B) Bright-field image of SLCs sorted by FACS. The arrowheads mark small round cells used for single-cell sequencing and ICSI. Scale bar, 50 μm.

(C) Bisulfite sequencing of DMRs of the imprinted genes *Snrpn* and *H19* in wild-type round spermatids and in vitro-derived SLCs. White and black circles indicate unmethylated and methylated CpGs, respectively. Values indicate percent methylation of all CpGs assessed.

(D) Unsupervised hierarchical clustering of ESCs, E12.5 male PGCs, day 6 PGCLCs, induced SLCs, and spermatids in vivo according to global gene expression.

(E) Live pups obtained by ICSI with PGCLC-derived SLCs. (i) and (ii) show one and five pups from two replicates, respectively.

(F) i and ii show genotyping for ESC-derived transgenes of (Ei) and (Eii), respectively. All pups were positive for *Prm1*-DsRed.

(G) Metaphase spread confirming the normal karyotype of the pup shown in (Ei).

(H) Bisulfite sequencing of *H19* and *Snrpn* DMRs in tail tip fibroblasts from the SLC-derived pup shown in (Ei) and a wild-type control.

See also Figures S4 and S5 and Table 1.

medium for EpiLC induction, resulted in the formation of PGCLCs that were capable of undergoing meiosis in vitro. This is supported by our findings from global transcription profiling, which revealed that the ESC-derived PGCLCs generated in our study clustered closely with E12.5 PGCs (Figure 4 D), a developmental stage close to entry into meiosis in vivo. In the mouse germline, female PGCs enter meiosis at E13.5 (McLaren, 2003). This is triggered by the release of endogenous RA from the mesonephros (Anderson et al., 2008). In contrast, in the male, initiation of meiosis remains suppressed until after birth (Zhou et al., 2008) because high levels of CYP26B1 expressed by somatic cells of the fetal male gonad degrade endogenous RA (Bowles et al., 2006; MacLean et al., 2007). Here we exposed PGCLCs resembling E12.5 PGCs to conditions supporting their entry into meiosis by identification of morphogens that induced upregulation of meiosis pathways and by providing a culture environment with postnatal somatic testicular cells expressing low CYP26B1 levels (Figure S3A).

We found that simultaneous exposure of PGCLCs to activin A, BMPs, and RA resulted in rapid silencing of *Blimp1* and *Stella* and subsequent upregulation of *Stra8* expression, resulting in initiation of meiosis and changes in gene expression that resemble those of in vivo differentiating germ cells (Figure 1; Kurimoto et al., 2008; Saitou et al., 2002). Consistent with previous observations demonstrating that BMPs and activin A are required for the self-renewal (Hu et al., 2004; Puglisi et al., 2004) and proliferation of neonatal germ cells (Mithraprabhu et al., 2010), our results also suggest that BMPs and activin A are essential for the proliferation of meiosis-competent PGCLCs in culture, whereas RA is required to induce regulatory networks that lead to meiotic entry and differentiation.

Under our culture conditions, the ESC-derived PGCLCs failed to differentiate into SSCs capable of self-renewal in vitro, evident

Table 1. Development of Embryos Generated via ICSI with In Vitro-Differentiated Haploid Spermatids

Origin of Sperm	Injected Oocytes (n)	Pronuclear Stage Embryos (n) (%)	Two-Cell Stage Embryos (n) (%)	Embryos Transferred (n)	Pups (n)	Pups Surviving to Adulthood (n)
Control	160	148 (92.5)	–	148	14	14
SGPD (1)	63	59 (93.6)	51 (86.4)	51	1	1
SGPD (2)	125	116 (92.8)	107 (92.2)	107	5	5
BVSC	191	171 (90)	159 (92.9)	159	3	3

See also Figure 5 and Figure S5.

from the absence of SSC-specific genes in PGCLC-derived germ cells. We presume that the in vitro culture system lacks features of the testicular microenvironment at the basement membrane required for SSC maintenance, including lack of growth factors required for SSC self-renewal, such as glial cell line-derived neurotropic factor (GDNF), bFGF, or EGF, among others (Kanatsu-Shinohara et al., 2003; Kanatsu-Shinohara and Shinohara, 2013; Kubota et al., 2004).

We observed that, during induction of meiotic differentiation in co-cultures, $KIT^{W}/KIT^{W\text{-}V}$ neonatal testicular cells formed colonies with PGCLCs by active cellular migration. Stimulated by RA, the PGCLCs synchronously passed a SSCs-like state and entered meiosis, reminiscent of PGCs in the E13.5 female genital ridge, which simultaneously enter meiosis at this stage (McLaren, 2003).

We found that differentiation of PGCLCs into male postmeiotic germ cells in vitro required simultaneous exposure to the sex hormones testosterone, FSH, and BPE. This reflects the dependence of in vivo spermatogenesis on pituitary FSH and locally produced testicular androgens, including testosterone. FSH supports Sertoli cell proliferation and stimulates mitotic division of spermatogonia, maintaining adequate cell counts (O'Shaughnessy, 2014). The requirement for BPE for spermatogenesis in vitro suggests that other pituitary factors promote meiotic progression and spermatid differentiation. These may include luteinizing hormone (LH), which normally stimulates the secretion of testosterone from Leydig cells but has also been implied in the maintenance of meiotic germ cells (O'Shaughnessy et al., 2009). The analysis and screening of pituitary tissues for factors affecting in vitro germ cell differentiation may further improve protocols for in vitro meiosis.

In summary, we demonstrate a robust approach toward the stepwise differentiation of pluripotent stem cells into haploid SLCs in vitro. The in vitro meiosis fully complies with the gold standards of meiosis, including erasure of imprints, synapsis, and recombination. Our findings could facilitate the generation of haploid human spermatids in vitro with the prospect of treating male infertility.

EXPERIMENTAL PROCEDURES

Derivation of BVSC and SGPD ESCs

BVSC transgenic mice (Ohinata et al., 2008) were provided by Mitinori Saitou. *Stra8*-EGFP transgenic mice and *Prm1*-DsRed transgenic mice were generated by pronuclear injection of *Stra8*-EGFP and *Prm1*-DsRed plasmids (Nayernia et al., 2006), a gift from Wolfgang Engel (University of Göttingen). ESCs were derived from blastocyst-stage embryos by standard culture on mouse feeder layers in 2i medium (Ying et al., 2008). For feeder-free culture, ESCs were maintained on dishes coated with poly-L-ornithine (0.01%; Sigma) and laminin (300 ng/ml, Invitrogen). All cell lines were negative for mycoplasma. All animal experiments were performed in compliance with the guidelines of the Institute of Zoology, Chinese Academy of Sciences.

Induction of EpiLCs and PGCLCs

Differentiation of ESCs into EpiLCs and PGCLCs was induced by culture conditions adapted from a protocol published previously with minor modifications (Hayashi et al., 2011). For EpiLC differentiation, 1×10^5 ESCs/well were plated in a 12-well plate coated with 16.7 μg/ml human plasma fibronectin in N2B27 medium supplemented with activin A, bFGF, and 1% knockout serum replacement (KSR). For PGCLC formation in floating culture, 2×10^3 EpiLCs/well were plated in a low cell-binding, U-bottom, 96-well plate (Corning Life Sciences) in modified N2B27 medium (N2B27 with 15% KSR, BMP-4, LIF, SCF, BMP-8a, and EGF). Cells were cultured in 5% CO_2 at 37°C. The medium was changed daily.

In Vitro Spermatogenesis

Testes of 2- to 8-day postpartum (dpp) Kit^{W}/ $Kit^{W\text{-}V}$ mice were harvested and digested by a two-step enzyme digestion method as described previously (Bellvé, 1993; Bellvé et al., 1977). Briefly, testes were dispersed with 1 mg/ml collagenase type IV at 37°C for 10 min, followed by digestion in 0.25% trypsin/1 mM EDTA for 10 min at 37°C. A single cell suspension was obtained after filtration through a 70-μm cell strainer, and cells were collected by centrifugation. PGCLCs were mixed with $Kit^{W}/Kit^{W\text{-}V}$ mouse testicular cells at a ratio of 1 to 1. From day 0 to day 6, cells were cultured in αMEM supplemented with 10% KSR, BMP-2/4/7 (20 ng/ml each, R&D Systems), retinoic acid (10^{-6} M, Sigma), and activin A (100 ng/ml, R&D Systems). From days 7–14, cells were cultured in αMEM containing 10% KSR, testosterone (10 μM, Acros Organics), FSH (200 ng/ml, Sigma), and BPE (50 μg/ml, Corning Life Sciences). The medium was changed every 2 days. Cells were cultured in 5% CO_2 at 37°C.

Immunostaining

Cells or seminiferous tubules were fixed for 15 min with 4% paraformaldehyde at room temperature, blocked for 30 min with 0.3% Triton X-100/2% BSA in PBS, and incubated with primary antibodies against OCT4 (Santa Cruz Biotechnology), NANOG (Millipore), SSEA1 (Millipore), DDX4 (Abcam), BLIMP1 (Abcam), STRA8 (Abcam), and GATA4 (Abcam). After overnight incubation at 4°C, samples were washed three times in PBS, followed by incubation with secondary antibodies or/and peanut agglutinin (PNA) (10 μg/ml, Sigma) for 1 hr. Secondary antibodies were labeled with fluorescein isothiocyanate (FITC), Cy3, and Cy5 (Jackson ImmunoResearch). DNA was counterstained with 10 μg/ml Hoechst 33342 for 15 min, followed by three washes with PBS. Images were captured with a Zeiss LSM780 Meta inverted confocal microscope.

Western Blotting

PGCLCs were collected into cell lysis buffer (10 mM Tris-HCl [pH 8.0], 10 mM NaCl, and 0.5% NP-40) containing protease inhibitor (Roche) for 30 min on ice. Lysates were centrifuged at 12,000 × *g* for 20 min at 4°C, and the resulting supernatants separated by electrophoresis and western blotting using antibodies against H3K27me3 (Millipore), H3K9me2 (Millipore), and H3 (Millipore).

Karyotype

After culture in medium supplemented with 0.025% colchicine for 6–8 hr, cells were subject to hypotonic treatment with 1% sodium citrate for 30 min at room temperature (RT), followed by fixation in freshly prepared methanol/acetic acid

(3:1) for 2 hr with three replacements of fixative. The coverslip was removed using dry ice. Chromosomes were visualized by Giemsa staining. Images were captured on a Leica DM 6000 B microscope.

DNA and RNA Isolation and Real-Time PCR

DNA and RNA from mouse tail tips or cell pellets were extracted with a MicroElute genomic DNA kit (OMEGA) or an RNeasy micro/mini kit (QIAGEN), respectively. Reverse transcription was performed using a QuantiTect reverse transcription kit (QIAGEN). PCR and real-time PCR were performed with gene-specific primers (Table S1). All gene expression analyses were performed with samples from three independent differentiation experiments.

Flow Cytometry Analysis

PGCLCs were dissociated in 0.25% trypsin/1 mM EDTA, re-suspended in PBS supplemented with 1% BSA, filtered through a 40-μm nylon mesh, and incubated with SSEA1-AF647-conjugated mouse monoclonal immunoglobulin M (IgM) (eBioscience) and Integrin β3-FITC-conjugated mouse monoclonal IgG1 (BioLegend) for 30 min at 37°C. For ploidy analysis, single-cell suspensions were stained with 10 μg/ml Hoechst 33342 for 20 min and washed three times with PBS. FACS analysis was performed using the FACS Calibur system (Becton Dickinson).

Bisulfite Sequencing

Sodium bisulfite treatment of DNA was performed using the EZ DNA methylation-direct kit (Zymo Research). PCR amplification was performed using hot start (HS) DNA polymerase (TAKARA) with specific primers for *H19* and *Snprn* DMR imprinting regions (Table S1). The PCR product was gel-extracted, subcloned into the pMD18T vector (TAKARA), and sequenced. The resulting data were analyzed using a web-based tool, Quantification Tool for Methylation Analysis (QUMA, http://quma.cdb.riken.jp/).

Chromosomal Spreads

Cultured cells were digested into single-cell suspensions. Chromosomal spreads were prepared using a hypotonic bursting technique (Peters et al., 1997). Primary antibodies were Sycp3 (Abcam), Sycp1 (Abcam), γH2AX (Abcam), Rad 51 (Santa Cruz), and Spo11 (provided by Scott Keeney) (Lange et al., 2011). Secondary antibodies were FITC-, Cy3-, Cy5-, and DyLight 405-labeled (Jackson ImmunoResearch). Images were captured with Zeiss LSM780 Meta inverted confocal microscope. Super-resolution analysis was performed using a Zeiss Elyra PS.1 microscope system.

Global Expression Analysis

Global transcription profiles of SSEA1/integrin β3 double-positive, day 6 PGCLCs, SSEA1/integrin β3 double-positive PGCs from male E12.5 fetuses, and individual sorted SLCs and spermatids were determined by microarray as described previously (NCBI GEO: GSE71478) (Zhao et al., 2009). Published ESC data (NCBI GEO: GSE16925) (Zhao et al., 2009) were used for unsupervised hierarchical clustering.

Intracytoplasmic Sperm Injection and Embryo Transfer

ICSI was performed as described previously (Li et al., 2012). SLCs were exposed to 5 μg/ml cytochalasin B in M2, and individual cells were injected into pre-activated mature oocytes with a Piezo-driven pipette, followed by culture in activation medium for 5 hr. Two-cell embryos were transferred to the oviduct of CD1 pseudopregnant females or further cultured to blastocyst stage in vitro, followed by embryo transfer into the uteri of recipient females. Full-term pups were delivered naturally or by cesarean section.

RRBS Library Preparation and Data Analysis

For RRBS, the libraries were generated and the data were analyzed as described previously (Gu et al., 2011; Shen et al., 2014; Yamaguchi et al., 2013). Paired-end sequencing was performed on an Illumina HiSeq 2500 sequencer (NCBI GEO: GSE76238). RRBS datasets of wild-type meiosis II (MII) oocyte and sperm were downloaded from the GEO database (GSE61331) (Shen et al., 2014). The sequencing reads were trimming by Trim Galore (Babraham Bioinformatics) with the "-rrbs" option and then mapped to the mouse genome (mm9 version) by Bismark v0.13.1 (Babraham Bioinformatics). The methylation levels of covered cytosine sites were calculated by dividing the number of reported C with the total number of reported C and T. Only the CpG sites that were covered by no less than ten reads were used for the next analysis. The hierarchical clustering was produced by the hcluster functions of R with the "euclidean" and "ward" Parameters. The Pearson correlation coefficients were generated using the lm function in R. The heatmaps were plotted by the heatmap.2 function in R. Histograms of methylation level distribution were drawn by ggplot2. Point plots were produced by the smoothScatter functions in R.

ACCESSION NUMBERS

The accession number for the RNA sequencing data reported in this paper is GEO: GSE71478. The accession number for the RRBS data reported in this paper is GEO: GSE76238.

SUPPLEMENTAL INFORMATION

Supplemental Information includes five figures, one table, and two movies and can be found with this article online at http://dx.doi.org/10.1016/j.stem.2016.01.017.

AUTHOR CONTRIBUTIONS

Conceptualization, X.-Y.Z., J.S., and Q.Z.; Methodology, Q.S.; Investigation, Q.Z., Y.Y., Y.Z., M.W., X.W., R.F., H.W., M.X., M.L., and X.G.; Data Curation, G.F.; Writing, M.L, X.G., X.-Y.Z., J.S., and Q.Z., with all authors approving the final version; Funding Acquisition, X.-Y.Z., J.S., and Q.Z.; Supervision, X.-Y.Z., J.S., and Q.Z.

ACKNOWLEDGMENTS

We thank Wolfgang Engel for the *Stra8*-EGFP and *Prm1*-DsRed plasmids, Mitinori Saitou for *Blimp1*-mVenus and *Stella*-ECFP (BVSC) transgenic mice, Scott Keeney for the SPO11 antibody, and Sigrid Eckardt and Xingxu Huang for help with manuscript preparation. This study was funded by the 973 Program (2011CB944304, 2012CBA01301, 2012CBA01300, and 2012CB966500).

Received: November 17, 2015
Revised: December 23, 2015
Accepted: January 21, 2016
Published: February 25, 2016

REFERENCES

Anderson, E.L., Baltus, A.E., Roepers-Gajadien, H.L., Hassold, T.J., de Rooij, D.G., van Pelt, A.M., and Page, D.C. (2008). Stra8 and its inducer, retinoic acid, regulate meiotic initiation in both spermatogenesis and oogenesis in mice. Proc. Natl. Acad. Sci. USA *105*, 14976–14980.

Aravind, L., Leipe, D.D., and Koonin, E.V. (1998). Toprim–a conserved catalytic domain in type IA and II topoisomerases, DnaG-type primases, OLD family nucleases and RecR proteins. Nucleic Acids Res. *26*, 4205–4213.

Bellvé, A.R. (1993). Purification, culture, and fractionation of spermatogenic cells. Methods Enzymol. *225*, 84–113.

Bellvé, A.R., Cavicchia, J.C., Millette, C.F., O'Brien, D.A., Bhatnagar, Y.M., and Dym, M. (1977). Spermatogenic cells of the prepuberal mouse. Isolation and morphological characterization. J. Cell Biol. *74*, 68–85.

Bowles, J., Knight, D., Smith, C., Wilhelm, D., Richman, J., Mamiya, S., Yashiro, K., Chawengsaksophak, K., Wilson, M.J., Rossant, J., et al. (2006). Retinoid signaling determines germ cell fate in mice. Science *312*, 596–600.

Eguizabal, C., Montserrat, N., Vassena, R., Barragan, M., Garreta, E., Garcia-Quevedo, L., Vidal, F., Giorgetti, A., Veiga, A., and Izpisua Belmonte, J.C. (2011). Complete meiosis from human induced pluripotent stem cells. Stem Cells *29*, 1186–1195.

Eijpe, M., Heyting, C., Gross, B., and Jessberger, R. (2000). Association of mammalian SMC1 and SMC3 proteins with meiotic chromosomes and synaptonemal complexes. J. Cell Sci. *113*, 673–682.

Geijsen, N., Horoschak, M., Kim, K., Gribnau, J., Eggan, K., and Daley, G.Q. (2004). Derivation of embryonic germ cells and male gametes from embryonic stem cells. Nature *427*, 148–154.

Gu, H., Smith, Z.D., Bock, C., Boyle, P., Gnirke, A., and Meissner, A. (2011). Preparation of reduced representation bisulfite sequencing libraries for genome-scale DNA methylation profiling. Nat. Protoc. *6*, 468–481.

Handel, M.A., Eppig, J.J., and Schimenti, J.C. (2014). Applying "gold standards" to in-vitro-derived germ cells. Cell *157*, 1257–1261.

Hayashi, K., Ohta, H., Kurimoto, K., Aramaki, S., and Saitou, M. (2011). Reconstitution of the mouse germ cell specification pathway in culture by pluripotent stem cells. Cell *146*, 519–532.

Hu, J., Chen, Y.X., Wang, D., Qi, X., Li, T.G., Hao, J., Mishina, Y., Garbers, D.L., and Zhao, G.Q. (2004). Developmental expression and function of Bmp4 in spermatogenesis and in maintaining epididymal integrity. Dev. Biol. *276*, 158–171.

Irie, N., Weinberger, L., Tang, W.W., Kobayashi, T., Viukov, S., Manor, Y.S., Dietmann, S., Hanna, J.H., and Surani, M.A. (2015). SOX17 is a critical specifier of human primordial germ cell fate. Cell *160*, 253–268.

Kanatsu-Shinohara, M., and Shinohara, T. (2013). Spermatogonial stem cell self-renewal and development. Annu. Rev. Cell Dev. Biol. *29*, 163–187.

Kanatsu-Shinohara, M., Ogonuki, N., Inoue, K., Miki, H., Ogura, A., Toyokuni, S., and Shinohara, T. (2003). Long-term proliferation in culture and germline transmission of mouse male germline stem cells. Biol. Reprod. *69*, 612–616.

Keeney, S., Giroux, C.N., and Kleckner, N. (1997). Meiosis-specific DNA double-strand breaks are catalyzed by Spo11, a member of a widely conserved protein family. Cell *88*, 375–384.

Koubova, J., Hu, Y.C., Bhattacharyya, T., Soh, Y.Q., Gill, M.E., Goodheart, M.L., Hogarth, C.A., Griswold, M.D., and Page, D.C. (2014). Retinoic acid activates two pathways required for meiosis in mice. PLoS Genet. *10*, e1004541.

Kubota, H., Avarbock, M.R., and Brinster, R.L. (2004). Growth factors essential for self-renewal and expansion of mouse spermatogonial stem cells. Proc. Natl. Acad. Sci. USA *101*, 16489–16494.

Kurimoto, K., Yabuta, Y., Ohinata, Y., Shigeta, M., Yamanaka, K., and Saitou, M. (2008). Complex genome-wide transcription dynamics orchestrated by Blimp1 for the specification of the germ cell lineage in mice. Genes Dev. *22*, 1617–1635.

Lammers, J.H., Offenberg, H.H., van Aalderen, M., Vink, A.C., Dietrich, A.J., and Heyting, C. (1994). The gene encoding a major component of the lateral elements of synaptonemal complexes of the rat is related to X-linked lymphocyte-regulated genes. Mol. Cell. Biol. *14*, 1137–1146.

Lange, J., Pan, J., Cole, F., Thelen, M.P., Jasin, M., and Keeney, S. (2011). ATM controls meiotic double-strand-break formation. Nature *479*, 237–240.

Li, W., Dou, Z.Y., Hua, J.L., and Wang, H.Y. (2007). [Activation of Stra 8 gene during the differentiation of spermatogonial stem cells]. Sheng Wu Gong Cheng Xue Bao *23*, 639–644.

Li, W., Shuai, L., Wan, H., Dong, M., Wang, M., Sang, L., Feng, C., Luo, G.Z., Li, T., Li, X., et al. (2012). Androgenetic haploid embryonic stem cells produce live transgenic mice. Nature *490*, 407–411.

MacLean, G., Li, H., Metzger, D., Chambon, P., and Petkovich, M. (2007). Apoptotic extinction of germ cells in testes of Cyp26b1 knockout mice. Endocrinology *148*, 4560–4567.

Mahadevaiah, S.K., Turner, J.M., Baudat, F., Rogakou, E.P., de Boer, P., Blanco-Rodríguez, J., Jasin, M., Keeney, S., Bonner, W.M., and Burgoyne, P.S. (2001). Recombinational DNA double-strand breaks in mice precede synapsis. Nat. Genet. *27*, 271–276.

McLaren, A. (2003). Primordial germ cells in the mouse. Dev. Biol. *262*, 1–15.

Menke, D.B., Koubova, J., and Page, D.C. (2003). Sexual differentiation of germ cells in XX mouse gonads occurs in an anterior-to-posterior wave. Dev. Biol. *262*, 303–312.

Meuwissen, R.L., Offenberg, H.H., Dietrich, A.J., Riesewijk, A., van Iersel, M., and Heyting, C. (1992). A coiled-coil related protein specific for synapsed regions of meiotic prophase chromosomes. EMBO J. *11*, 5091–5100.

Mithraprabhu, S., Mendis, S., Meachem, S.J., Tubino, L., Matzuk, M.M., Brown, C.W., and Loveland, K.L. (2010). Activin bioactivity affects germ cell differentiation in the postnatal mouse testis in vivo. Biol. Reprod. *82*, 980–990.

Nayernia, K., Nolte, J., Michelmann, H.W., Lee, J.H., Rathsack, K., Drusenheimer, N., Dev, A., Wulf, G., Ehrmann, I.E., Elliott, D.J., et al. (2006). In vitro-differentiated embryonic stem cells give rise to male gametes that can generate offspring mice. Dev. Cell *11*, 125–132.

Neale, M.J., and Keeney, S. (2006). Clarifying the mechanics of DNA strand exchange in meiotic recombination. Nature *442*, 153–158.

O'Shaughnessy, P.J. (2014). Hormonal control of germ cell development and spermatogenesis. Semin. Cell Dev. Biol. *29*, 55–65.

O'Shaughnessy, P.J., Morris, I.D., Huhtaniemi, I., Baker, P.J., and Abel, M.H. (2009). Role of androgen and gonadotrophins in the development and function of the Sertoli cells and Leydig cells: data from mutant and genetically modified mice. Mol. Cell. Endocrinol. *306*, 2–8.

Ohinata, Y., Sano, M., Shigeta, M., Yamanaka, K., and Saitou, M. (2008). A comprehensive, non-invasive visualization of primordial germ cell development in mice by the Prdm1-mVenus and Dppa3-ECFP double transgenic reporter. Reproduction *136*, 503–514.

Peters, A.H., Plug, A.W., van Vugt, M.J., and de Boer, P. (1997). A drying-down technique for the spreading of mammalian meiocytes from the male and female germline. Chromosome Res. *5*, 66–68.

Puglisi, R., Montanari, M., Chiarella, P., Stefanini, M., and Boitani, C. (2004). Regulatory role of BMP2 and BMP7 in spermatogonia and Sertoli cell proliferation in the immature mouse. Eur. J. Endocrinol. *151*, 511–520.

Saitou, M., Barton, S.C., and Surani, M.A. (2002). A molecular programme for the specification of germ cell fate in mice. Nature *418*, 293–300.

Seki, Y., Hayashi, K., Itoh, K., Mizugaki, M., Saitou, M., and Matsui, Y. (2005). Extensive and orderly reprogramming of genome-wide chromatin modifications associated with specification and early development of germ cells in mice. Dev. Biol. *278*, 440–458.

Shen, L., Inoue, A., He, J., Liu, Y., Lu, F., and Zhang, Y. (2014). Tet3 and DNA replication mediate demethylation of both the maternal and paternal genomes in mouse zygotes. Cell Stem Cell *15*, 459–470.

Sun, Y.C., Cheng, S.F., Sun, R., Zhao, Y., and Shen, W. (2014). Reconstitution of gametogenesis in vitro: meiosis is the biggest obstacle. Yi Chuan Xue Bao *41*, 87–95.

Yamaguchi, S., Shen, L., Liu, Y., Sendler, D., and Zhang, Y. (2013). Role of Tet1 in erasure of genomic imprinting. Nature *504*, 460–464.

Ying, Q.L., Wray, J., Nichols, J., Batlle-Morera, L., Doble, B., Woodgett, J., Cohen, P., and Smith, A. (2008). The ground state of embryonic stem cell self-renewal. Nature *453*, 519–523.

Yokonishi, T., Sato, T., Katagiri, K., Komeya, M., Kubota, Y., and Ogawa, T. (2013). In vitro reconstruction of mouse seminiferous tubules supporting germ cell differentiation. Biol. Reprod. *89*, 15.

Zhao, X.Y., Li, W., Lv, Z., Liu, L., Tong, M., Hai, T., Hao, J., Guo, C.L., Ma, Q.W., Wang, L., et al. (2009). iPS cells produce viable mice through tetraploid complementation. Nature *461*, 86–90.

Zhou, Q., Li, Y., Nie, R., Friel, P., Mitchell, D., Evanoff, R.M., Pouchnik, D., Banasik, B., McCarrey, J.R., Small, C., and Griswold, M.D. (2008). Expression of stimulated by retinoic acid gene 8 (Stra8) and maturation of murine gonocytes and spermatogonia induced by retinoic acid in vitro. Biol. Reprod. *78*, 537–545.